Quantum phase dynamics of an initially one-mode amplitude-squeezed field interacting with a two-state molecular system

ARTICLE *in* CHEMICAL PHYSICS LETTERS · APRIL 1999

Impact Factor: 1.9 · DOI: 10.1016/S0009-2614(99)00322-X

2 AUTHORS, INCLUDING:

Masayoshi Nakano
Osaka University
337 PUBLICATIONS **4,781** CITATIONS

Numerical Coupled Liouville Approach: Application to Second Hyperpolarizability of Molecular Aggregate

M. NAKANO, S. YAMADA, H. NAGAO, K. YAMAGUCHI

Department of Chemistry, Graduate School of Science, Osaka University, Toyonaka, Osaka 560, Japan

Received 17 March 1998; revised 10 July 1998; accepted 14 July 1998

ABSTRACT: In our previous study [Int. J. Quant. Chem., to appear], we have developed a novel numerical calculation scheme for a dynamics of quantum network for linear molecular aggregates under intense time-dependent electric fields. In this approach, each molecule is assumed to be an electric dipole arranged linearly with an angle from the longitudinal axis, and the molecular interactions are taken into account by adding the radiations from these dipoles to the external electric fields. The effects of the radiations from all the dipoles involve the intermolecular distance, the speed of light, retarded polarization, and its first- and second-order time derivatives at the position of each dipole. The quantum dynamics is performed by solving coupled Liouville equations composed of the Liouville equation for each dipole. In the present study, we develop a calculation approach of nonperturbative second hyperpolarizability γ in our novel approach and examine the γ of dimer models composed of two-state molecules under the one-photon near resonant intense laser fields. Similar phase transition-like behavior in the field-intensity dependence of the γ is observed. We also investigate the second hyperpolarizability spectra in the three-photon resonant region for dimers composed of three-state molecules, which mimic the electronic states of allyl cation. Contrary to the one-photon resonant case, phase transition-like behavior is not observed in the intensity dependence of γ in the three-photon resonant region. Int J Quant Chem 71: 295–306, 1999

Key words: hyperpolarizability; molecular aggregate; Liouville equation; nonlinear optics; optical retardation; three-photon resonance

Correspondence to: M. Nakano.

Contract grant sponsor: Ministry of Education, Science and Culture of Japan.

Contract grant numbers: 09241218, 10149101.

Contract grant sponsor: INAMORI Foundation.

CCC 0020-7608 / 99 / 040295-12

Introduction

Hyperpolarizability plays a significant role in characterizing and understanding a variety of intermolecular interactions and light–matter interactions, especially those concerning nonlinear optical processes [1, 2]. Particularly the second hyperpolarizability γ has attracted much attention since it determines various third-order nonlinear optical properties, which are essential for many applications in optoelectronics. A lot of experimental and theoretical studies have been performed in order to analyze the mechanism of nonlinear optical processes and to elucidate the structure–property relations for nonlinear optical substances. Many features of γ for small-size organic molecules, including closed- and open-shell π-conjugated compounds, have been fruitfully accounted for by using quantum chemical calculations [3].

On the other hand, in recent years much effort has been devoted to an analysis of quantum dynamical properties of low-dimensional mesoscopic-size systems such as molecular aggregates and many attracting features, e.g., the enhancement of linear and nonlinear optical responses [4], superradiance [5], and intrinsic optical bistability [6], have been revealed. These features originate in the collective characters of the aggregate wavefunctions. In our previous study [7], we have developed a novel numerical calculation approach, which is referred to as the numerical coupled Liouville approach (NCLA), to quantum dynamics for linear molecular aggregates. In this approach, we treat the intermolecular interactions by considering mutual propagation of retarded optical fields generated by each molecule, instead of considering static dipole–dipole interactions. This approach can describe the quantum dynamics for aggregates without electron exchanges among monomers and has advantages in a remarkable reduction of the amount of calculations and in describing the long-distance intermolecular interactions where optical retardation effects becomes important [8]. The optical retardation effects are also considered to be an essential factor of optical bistability effects [9] for mesoscopic-size aggregates. From the previous results for dimers composed of two-state monomers under a one-photon resonant external electric field [7], the population and polarization changes are found to exhibit a phase transition-like behavior as the intensity of external field increases. This feature is considered to be related to the feedback effects of the retarded fields on the each molecule.

On the analogy of these behaviors in population and polarizability, the nonlinear optical properties are also expected to exhibit some attracting behaviors with respect to the increasing field intensity. In this study, therefore, the γ values for the linear aggregates under intense electric fields are investigated. In order to describe the nonlinear optical responses of substances under intense fields, we have to consider some nonperturbative features of hyperpolarizability. Usually, a calculation of hyperpolarizabilities is performed by the perturbative approach [3]. In that case, the response of a system interacting with an external field can be expanded as a power series in that field. For intense applied fields that cause a saturation of the transitions, however, it is found that the perturbative expansion approach breaks down and that another definition of the response based on the nonperturbative approach [10–14] is needed. In such a case, the hyperpolarizabilities become intensity dependent, and the various nonlinear optical phenomena originating in the intensity-dependent hyperpolarizabilities appear. For example, the multiphoton absorption peaks, the higher-order (up to 27th order) nonlinear wave mixing [15], and the power dependence of the phase conjugated signal of a degenerate four-wave mixing (DFWM) using an organic dye [16] have been detected. These recent experimental studies indicate that the perturbative approach is not sufficient and the nonperturbative one is essential for the description of the intensity-dependent hyperpolarizabilities. In this study, our calculation procedure of nonperturbative hyperpolarizabilities by using the numerical Liouville approach (NLA) [14] are extended to the case of NCLA.

First, we briefly explain a quantum electrodynamical formalism for molecular aggregates coupled with external electric fields. We employ the semiclassical approximation, in which the interaction terms between monomer and field are considered classically. The definition and calculation procedure of nonperturbative hyperpolarizability are explained in the NCLA. Second, the nonperturbative γ in the one-photon resonant region is investigated for a dimer model constructed from two-state molecules, and its dependence on the intermolecular distance and external field intensity is elucidated. The spectra of γ is also investigated in

comparison with that of the monomer. In this study, we consider the γ in the third-harmonic generation (THG) [2], which is especially important for an application to nonlinear optoelectronics. In this case, the three-photon resonance, which hardly causes population changes in the excited states, also appears. The intensity and molecular distance dependences of γ in the three-photon resonance region are investigated and are discussed in comparison with the case of one-photon resonant γ.

Methodology

SEMICLASSICAL HAMILTONIAN FOR FIELD-MOLECULE COUPLED SYSTEM

In this section, we explain the semiclassical Hamiltonian for molecular aggregates under electric fields. In semiclassical approach, molecules are treated quantum mechanically, while fields are taken to be classical time-dependent fields. As a result, the field part Hamiltonian disappears. This semiclassical treatment is found to be acceptable for the case of intense external fields. The semiclassical Hamiltonian is expressed by Eqs. (1), (2), and (3) [8]:

$$H = H_{\mathrm{mol}} + H_{\mathrm{int}}, \tag{1}$$

where the Hamiltonian of molecular part is

$$H_{\mathrm{mol}} = \sum_{\zeta} \left\{ \frac{1}{2m} \sum_{\alpha} \mathbf{p}_{\alpha}^{2}(\zeta) + V(\zeta) \right\}, \tag{2}$$

and the interaction part between semiclassical fields and molecules is

$$H_{\mathrm{int}} = -\frac{1}{\varepsilon_0} \sum_{\zeta} \boldsymbol{\mu}(\zeta) \cdot \mathbf{d}^{\perp}(\mathbf{R}_{\zeta}). \tag{3}$$

Here, ζ indicates the molecule ζ. In Eq. (2), $(1/2m)\Sigma_{\alpha}\mathbf{p}_{\alpha}^{2}(\zeta)$ and $V(\zeta)$ represent the kinetic and the intramolecular Coulomb potential parts of molecule ζ, respectively. In Eq. (3), the $\mathbf{d}^{\perp}(\mathbf{R}_{\zeta})$ involves the classical external electric fields acting on the molecule ζ plus the fields induced by the rest of the molecules. We can recognize that the Eq. (3) does not involve the Coulomb static potential for the intermolecular interaction and only involves the interactions between dipole moment $\boldsymbol{\mu}(\zeta)$ and the field $\mathbf{d}^{\perp}(\mathbf{R}_{\zeta})$, which is fully retarded. This intermolecular interaction can be described by exchange of transverse photons in quantum electrodynamics, while in the semiclassical approach, this is described by a propagation of classical time-dependent fields.

Usually, the intermolecular interactions are treated by including instantaneous electrostatic interactions, i.e., dipole–dipole coupling. However, only including these interactions cannot describe the optical retardation effects, which are essential for describing wave–zone intermolecular interactions [8]. Therefore, the semiclassical approach using Eqs. (1)–(3) is expected to be suitable for investigating nonlinear optical responses of mesoscopic (intermediate)-size molecular aggregates interacting with intense external fields.

DENSITY MATRIX FORMALISM FOR ONE-DIMENSIONAL MOLECULAR AGGREGATES UNDER INTENSE ELECTRIC FIELDS

The time evolution of a molecular system is described by the following density matrix equation [13]:

$$i\hbar \frac{\partial}{\partial t}\rho(t) = [H(t), \rho(t)] - i\Gamma\rho(t), \tag{4}$$

where $\rho(t)$ indicates the total molecular density matrix and the second term in the right-hand side of Eq. (4) represents relaxation processes in Markoff approximation. As mentioned in the above section, the total Hamiltonian $H(t)$ is expressed by the sum of the one-molecule Hamiltonian $H^{(\zeta)}(t)$, as follows:

$$H(t) = \sum_{\zeta}^{N} H^{(\zeta)}(t), \tag{5}$$

where

$$\begin{aligned} H^{(\zeta)}(t) &= H_{\mathrm{mol}}^{(\zeta)}(t) + H_{\mathrm{int}}^{(\zeta)}(t) \\ &= \frac{1}{2m} \sum_{\alpha} \mathbf{p}_{\alpha}^{(\zeta)2} + V^{(\zeta)} - \boldsymbol{\mu}^{(\zeta)} \cdot \mathbf{E}^{(\zeta)}. \end{aligned} \tag{6}$$

In this case, the Eq. (4) can be reduced to each one-molecule density matrix equation [7] expressed by

$$i\hbar \frac{\partial}{\partial t}\rho^{(\zeta)}(t) = [H^{(\zeta)}(t), \rho^{(\zeta)}(t)] - i\Gamma\rho^{(\zeta)}(t). \tag{7}$$

The intermolecular interaction is considered by the electric field involving not only external fields but

also the fields induced by the rest of the molecular aggregates. In this study, we consider the linear molecular aggregate shown in Figure 1. Each molecule is assumed to be a dipole separated by a distance $r_{\zeta\zeta'} = |\mathbf{r}_\zeta - \mathbf{r}_{\zeta'}|$ and having an angle θ between the dipole and the longitudinal axis. This approximation is considered to be accepted in the case with an intermolecular distance larger than the size of the element molecule.

Suppose that an aggregate is composed of identical N molecules and each molecule is constructed by M states, the matrix representation of Eq. (7) is expressed as

$$\begin{aligned}\dot{\rho}_{ij}^{(\zeta)}(t) = & -i(1-\delta_{ij})E_{ij}\rho_{ij}^{(\zeta)}(t) \\ & - i\sum_{k}^{M}\left(H_{\mathrm{int}\,ik}^{(\zeta)}(t)\rho_{kj}^{(\zeta)}(t)\right. \\ & \left.-\rho_{ik}^{(\zeta)}(t)H_{\mathrm{int}\,kj}^{(\zeta)}(t)\right) \\ & -(\Gamma\rho^{(\zeta)}(t))_{ij}. \end{aligned} \tag{8}$$

Here, the $E_{ij}(\equiv E_i - E_j)$ is the transition energy, and $\rho^{(\zeta)}(t)$ is the density matrix of the molecule ζ. The interaction term $H_{\mathrm{int}}^{(\zeta)}(t)$ involves the electric field $\mathbf{E}^{(\zeta)}$ acting on the molecule ζ. This field $\mathbf{E}^{(\zeta)}$ is expressed as [9]

$$\mathbf{E}^{(\zeta)} = \mathbf{E}^{\mathrm{ext}(\zeta)} + \sum_{\zeta'\neq\zeta}^{N}\mathbf{E}^{(\zeta\zeta')}, \tag{9}$$

where the first term is external electric field $\mathbf{E}^{\mathrm{ext}(\zeta)}$ and the second term is the field induced by the rest of the aggregates in the position ζ. The incident field is assumed to be a plane wave with frequency ω and wave vector $\mathbf{k}$ traveling perpendicular to the longitudinal axis and the polarization vector is parallel to the dipole vector, so that the $\mathbf{E}^{\mathrm{ext}(\zeta)} = \mathbf{E}^{\mathrm{ext}}$ for arbitrary ζ. The field induced by the molecule ζ' is regarded as the classical field radiated by the a classical dipole, so that the $\mathbf{E}^{(\zeta\zeta')}(t)$ is represented by [17]

$$\begin{aligned}\mathbf{E}^{(\zeta\zeta')}(t) = & \left[\frac{3p^{(\zeta')}(t')}{r_{\zeta'\zeta}^5} + \frac{3\dot{p}^{(\zeta')}(t')}{cr_{\zeta'\zeta}^4} + \frac{\ddot{p}^{(\zeta')}(t')}{c^2r_{\zeta'\zeta}^3}\right] \\ & \times(\mathbf{n}\cdot\mathbf{r}_{\zeta'\zeta})\mathbf{r}_{\zeta'\zeta} \\ & -\left[\frac{p^{(\zeta')}(t')}{r_{\zeta'\zeta}^3} + \frac{\dot{p}^{(\zeta')}(t')}{cr_{\zeta'\zeta}^2} + \frac{\ddot{p}^{(\zeta')}(t')}{c^2r_{\zeta'\zeta}}\right]\mathbf{n} \\ \equiv & f(t')(\mathbf{n}\cdot\mathbf{r}_{\zeta'\zeta})\mathbf{r}_{\zeta'\zeta} - f_2(t')\mathbf{n}, \end{aligned} \tag{10}$$

where $t' = t - r_{\zeta'\zeta}/c$, $\mathbf{n} = \boldsymbol{\mu}/\mu$, and $\mathbf{r}_{\zeta'\zeta} = (\zeta' - \zeta)\mathbf{a}$. The polarization $p^{(\zeta')}(t')$ and its time derivatives, $\dot{p}^{(\zeta')}(t')$ and $\ddot{p}^{(\zeta')}(t')$, are calculated quantum mechanically. These quantities are shown to be fully retarded. Suppose that an external field is a continuous-wave laser

$$\mathbf{E}^{ext}(t) = \mathbf{F}\cos\omega t = \frac{\mathbf{F}}{2}(e^{i\omega t} + e^{-i\omega t}), \tag{11}$$

the interaction term $H_{\mathrm{int}\,ik}^{(\zeta)}(t)$ is expressed using Eqs. (9) and (10) as

$$\begin{aligned}H_{\mathrm{int}\,ik}^{(\zeta)}(t) = & -\boldsymbol{\mu}_{ik}\cdot\mathbf{E}^{(\zeta)}(t) \\ = & -\boldsymbol{\mu}_{ik}\cdot\mathbf{E}^{\mathrm{ect}}(t) - \sum_{\zeta'\neq\zeta}^{N}\boldsymbol{\mu}_{ik}\cdot\mathbf{E}^{(\zeta'\zeta)}(t) \\ = & -\boldsymbol{\mu}_{ik}\left(F\cos\omega t\right. \\ & \left.+\sum_{\zeta'\neq\zeta}^{N}\left[f_1(t')(r_{\zeta'\zeta}\cos\theta)^2 - f_2(t')\right]\right) \\ \equiv & -\mu_{ik}E_\zeta(t). \end{aligned} \tag{12}$$

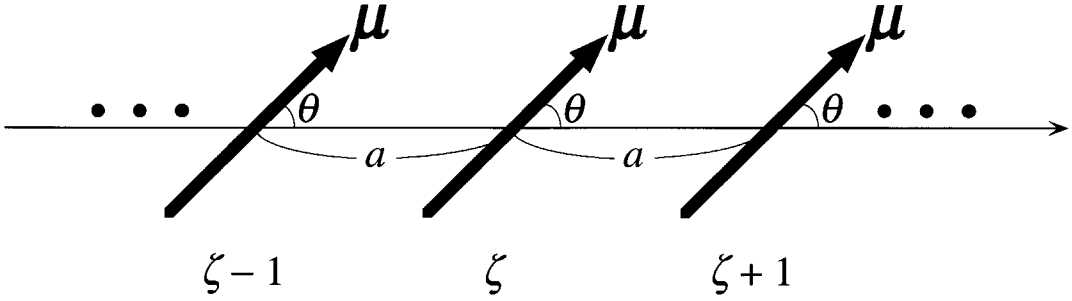

FIGURE 1. Schematic diagram of linear molecular aggregate. The arrow represents the direction of the dipole of the one-molecular system aligned with angle θ from the longitudinal axis. These molecules are separated each other by the distance a.

The relaxation term $-(\Gamma\rho^{(\zeta)}(t))_{ij}$ in Eq. (8) can be considered as the following two types of mechanisms [13]:

$$-(\Gamma\rho^{(\zeta)}(t))_{ii} = -\Gamma_{ii}\,\rho_{ii}^{(\zeta)}(t) + \sum_{m\neq i}^{M}\gamma_{mi}\,\rho_{mm}^{(\zeta)}(t), \tag{13}$$

and

$$-(\Gamma\rho^{(\zeta)}(t))_{ij} = -\Gamma_{ij}\,\rho_{ij}^{(\zeta)}(t). \tag{14}$$

Here, we assume the damping parameters are identical for all the molecules. Equations (13) and (14) describe population and coherent damping mechanisms, respectively. The $\gamma_{ij}(\neq\gamma_{ji})$ represents a feeding parameter. The off-diagonal damping parameter is expressed as

$$\Gamma_{ij} = \tfrac{1}{2}(\Gamma_{ii}+\Gamma_{jj}) + \Gamma'_{ij}, \tag{15}$$

and

$$\Gamma_{ij} = \Gamma_{ji}, \tag{16}$$

where Γ'_{ij} is the pure dephasing factor. In this study, we assume a closed system, and then the factor γ_{ij} is related to the decay rate as

$$\Gamma_{ii} = \sum_{l\neq i}^{M}\gamma_{il}. \tag{17}$$

We perform a numerically exact calculation treating the aggregates with arbitrary number of molecules with any M states. The Eq. (8) is solved in a numerically exact manner by using the sixth-order Runge–Kutta method. To perform this time evolution, we have to calculate the electric field $E_\zeta(t)$ acting on the molecule ζ at each time step. From Eq. (10), the $E_\zeta(t)$ includes the polarizability $p^{(\zeta')}(t')$ and its time derivatives, $\dot{p}^{(\zeta')}(t')$ and $\ddot{p}^{(\zeta')}(t')$, for the molecules at the different position $(\zeta'\neq\zeta)$ at the past time $t'(=t-r_{\zeta\zeta'}/c)$. The $p^{(\zeta')}(t')$ is calculated quantum mechanically by

$$p^{(\zeta')}(t') = \sum_{i,j}^{M}\mu_{ij}\,\rho_{ji}^{(\zeta')}(t'), \tag{18}$$

and the $\dot{p}^{(\zeta')}(t')$ and $\ddot{p}^{(\zeta')}(t')$ are calculated by using the numerical differentiation formulas:

$$\dot{p}^{(\zeta')}(t') = \frac{p^{(\zeta')}(t'+\Delta t) - p^{(\zeta')}(t'-\Delta t)}{2\,\Delta t}, \tag{19}$$

and

$$\ddot{p}^{(\zeta')}(t') = \frac{p^{(\zeta')}(t'+\Delta t) - 2\,p^{(\zeta')}(t') + p^{(\zeta')}(t'-\Delta t)}{(\Delta t)^2}. \tag{20}$$

Here, Δt is a minimum interval of time determined by $\Delta t = T/L$, where T is a period of the external field and L is a division number of the period. The population averaged over the molecular aggregate is presented by

$$p_{il}^{\mathrm{av}}(t) = \frac{\sum_{\zeta}^{N}\rho_{ii}^{(\zeta)}(t)}{N}. \tag{21}$$

It is noted that we have to store the past polarizabilities for each molecule ζ in order to calculate the E_ζ including optical retardation effects.

The procedure of the NCLA is shown in Figure 2. The NCLA includes the five steps. It is noted that the procedure has a feedback effect, i.e., polarization $p^{(\zeta')}(t')$ for molecules ζ' at the time t' are used to calculate the field $E^{(\zeta)}(t)$ acting on the molecule ζ at the time $t(>t')$. This feedback effect is considered to cause various collective phenomena, e.g., intrinsic optical bistability [7].

NONPERTURBATIVE SECOND HYPERPOLARIZABILITY

In this section, we briefly explain our definition of the nonperturbative (intensity-dependent) γ. The nonlinear optical response of an ensemble of systems to the external electric fields is represented by a macroscopic polarization density $\mathbf{P}(t)$, which can be written with the dipole moment operator $\boldsymbol{\mu}$ and density matrix operator $\rho(t)$ as

$$\mathbf{P}(t) = \mathrm{Tr}[\boldsymbol{\mu}\,\rho(t)]. \tag{22}$$

The macroscopic polarization density $\mathbf{P}(t)$ can be expanded as a Fourier series in the external frequencies in the steady state as follows:

$$\mathbf{P}(t) = \sum_{m_1,m_2,\ldots,m_M}\mathbf{P}_{m_1\ldots m_M}(\omega) \times e^{-i(m_1\omega_1+\cdots+m_M\omega_M)t}. \tag{23}$$

Here, $\mathbf{P}_{m_1\ldots m_M}(\omega)$ is the Fourier component at frequency $\omega = m_1\omega_1 + m_2\omega_2 + \cdots + m_M\omega_M$.

The THG is considered as an example. The γ in other nonlinear optical phenomena can be calcu-

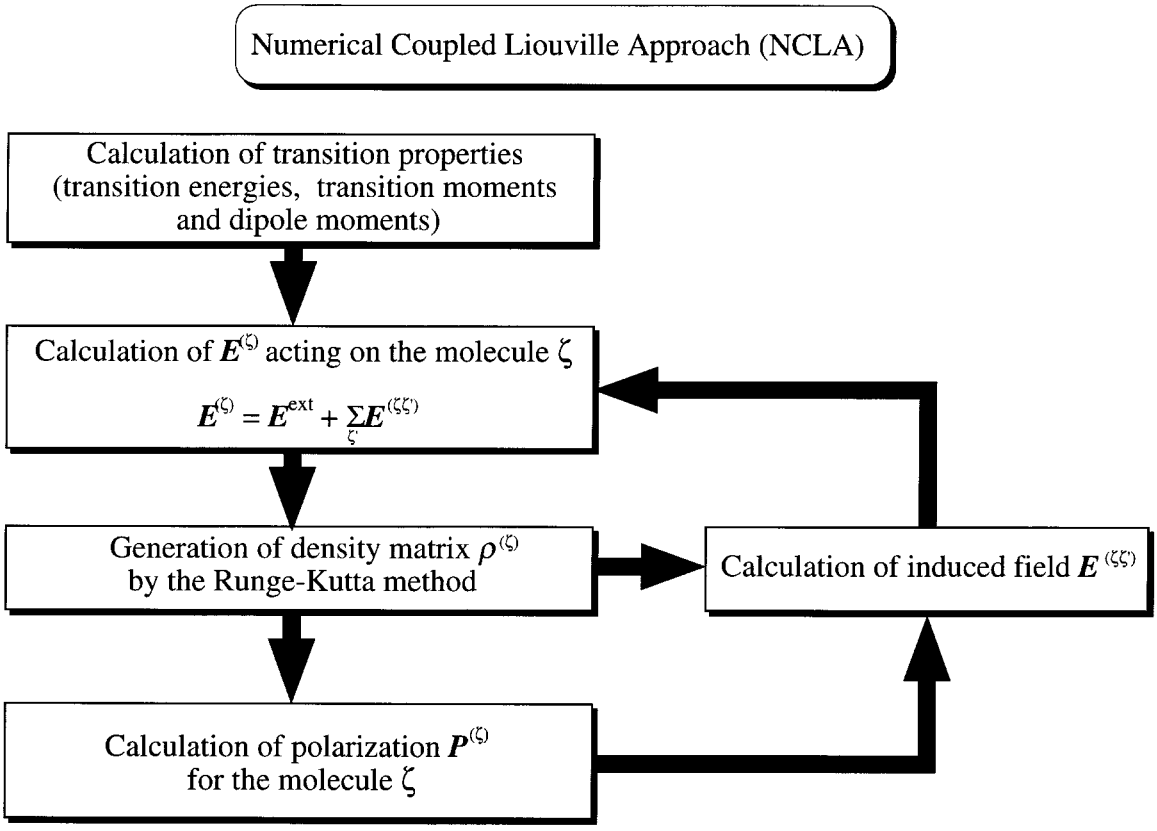

FIGURE 2. Schematic diagram describing the process of the numerical coupled Liouville approach (NCLA).

lated similarly [18]. In the THG process, the polarization with a frequency 3ω is induced in the system by three incident beams with an amplitude $\varepsilon(\omega)$, which is regarded as a real number in this work, and a frequency ω. The third-harmonic response $\mathbf{P}(3\omega)$ can be expressed by using the lth-order perturbative polarizability $\chi^{(l)}$ as follows:

$$\begin{aligned}\mathbf{P}(3\omega) &= \mathbf{P}_{111}(3\omega) + \mathbf{P}_{210}(3\omega) + \mathbf{P}_{120}(3\omega) \\ &\quad + \mathbf{P}_{012}(3\omega) + \mathbf{P}_{021}(3\omega) \\ &\quad + \mathbf{P}_{201}(3\omega) + \mathbf{P}_{102}(3\omega) + \cdots \\ &= 27\chi^{(3)}(-3\omega;\omega,\omega,\omega)\varepsilon^3(\omega) + \cdots. \quad (24)\end{aligned}$$

Here, the Fourier components $\mathbf{P}_{m_1m_2m_3}(3\omega)$ satisfy the condition $m_1 + m_2 + m_3 = 3$. The nonperturbative second hyperpolarizability $\chi_g^{(3)}(3\omega)$ in THG can be defined as [14]

$$\chi_g^{(3)}(3\omega)(\mathrm{THG}) = \frac{\mathbf{P}(3\omega)}{27\boldsymbol{\varepsilon}^3(\omega)} = \frac{\mathbf{P}'(3\omega)}{\boldsymbol{\varepsilon}'^3(\omega)}, \quad (25)$$

where $\varepsilon'(\omega)(\equiv 3\varepsilon(\omega))$ and $\mathbf{P}'(3\omega)(\equiv \mathbf{P}(3\omega))$ are obtained by the Fourier transformation of incident electric field and induced polarization time series, respectively. As can be seen from Eqs. (24) and (25), for weak incident fields, the nonperturbative (intensity-dependent) $\chi_g^{(3)}(3\omega)$ can reduce to the perturbative (intensity-independent) $\chi^{(3)}(-3\omega;\omega,\omega,\omega)$. In contrast, for strong incident fields, the intensity-dependent terms involving higher-order polarizabilities ($\chi^{(5)}, \chi^{(7)}, \ldots$, etc.) can contribute to $\chi_g^{(3)}(3\omega)$ significantly. The $\chi_g^{(3)}(3\omega)$ is referred to as $\gamma(3\omega)$ hereafter.

The polarization of molecule ζ, $p^{(\zeta)}(t)$, is transformed to the $p^{\zeta)}(\omega)$ in frequency domain by using the following discrete Fourier transformation:

$$p^{(\zeta)}(\omega_j) = \frac{1}{n}\sum_{k=0}^{n-1} p^{(\zeta)}(t_k)\exp\left[i\left(\frac{2\pi}{n}jk\right)\right]$$
$$(j = 0,1,\ldots,n-1; k = 0,1,\ldots,n-1). \quad (26)$$

Here, the used number of time-series data is n, the kth discrete time is $t_k = (L/n)k$, and the jth discrete frequency is $\omega_j = (2\pi/L)j$ where the mini-

mum t value (t_0) is 0 and the maximum t value (t_{n-1}) is L. Using Eq. (25), the nonperturbative second hyperpolarizability $\gamma(3\omega)$ for a molecular aggregate is calculated by

$$\gamma(3\omega) = \frac{\sum_{\zeta=1}^{N} p^{(\zeta)}(3\omega)}{27\varepsilon^3(\omega)}. \qquad (27)$$

In this study, $\varepsilon(\omega)$ is $F/6$ since we use the field $\varepsilon(= F/2)$ [see Eq. (11)] composed of three identical electric fields. For intense external fields, this quantity can exhibit various intensity-dependent phenomena such as a spectral broadening, and a displacement and an appearance of new resonance peak [18].

Results and Discussion

VARIATIONS IN γ IN ONE-PHOTON RESONANT REGION OF A DIMER MODEL FOR INTERMOLECULAR DISTANCES AND FIELD INTENSITIES

In this section, we investigate the γ of an artificial dimer model composed of the two-state one-molecule systems shown in Figure 3. The damping factor Γ_{22} is determined by a energy-dependent relation: $\Gamma_{22} = fE_{21}(f = 0.02)$ [19]. The external single-mode laser has a frequency (37,787 cm^{-1}) as compared to the one-photon resonant frequency (37,800 cm^{-1}) for the two-state one-molecule model. The division number of the one optical cycle of the external field is 1000, and the γ is calculated by using the Fourier transformation of polarization for 100 optical cycles after nonstationary time evolution (400 cycles). As an example, we consider a case of angle 90° between the dipole for each molecule and the longitudinal axis. This corresponds to the case of the H aggregate [4].

The dependence of the γ on the applied field intensities are investigated for this dimer model. Figure 4 shows the results at seven intermolecular distances: (a) infinite, (b) 80 a.u., (c) 60 a.u., (d) 50 a.u., (e) 40 a.u., (f) 30 a.u., and (g) 25 a.u. The result of case (a) is obtained by using noninteracting dimer model. As shown in Figure 4, the γ values for cases (a)–(e) are found to increase with the decrease in the intermolecular distance in the low field-intensity region (around 5.0×10^3 MW/cm^2), while those for cases (f) and (g) are found to be reduced in the same region. However, the γ values for cases (f) and (g) show abrupt increases at 5.0×10^3 and 1.3×10^4 MW/cm^2, respectively. Similar to the abrupt population differences observed in our previous study [7], the γ value is found to exhibit an abrupt change around the same intermolecular distance.

These abrupt changes in the γ in the one-photon resonant region under the high-intensity field are considered to originate in the retarded intermolecular interaction. A feedback effect involved

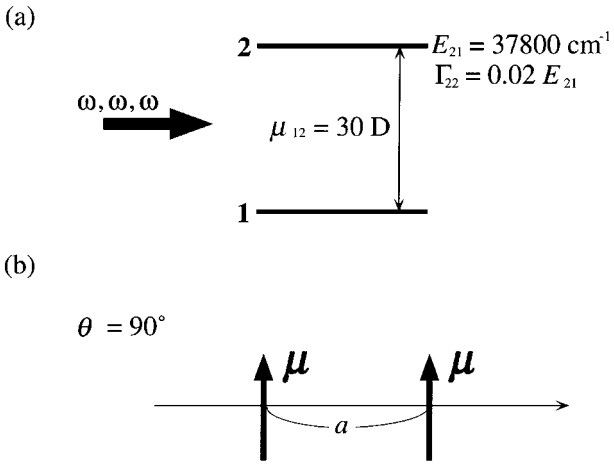

FIGURE 3. Two-state model (constructed from ground (**1**) and the excited (**2**) states) for (a) one-molecule system. (b) The dimer with $\theta = 90°$ is considered. The transition moment is $\mu_{12} = 30$ D, the transition energy is $E_{21} = 37{,}800$ cm^{-1}, and the damping factor is $\Gamma_{22} = fE_{21}(f = 0.02)$.

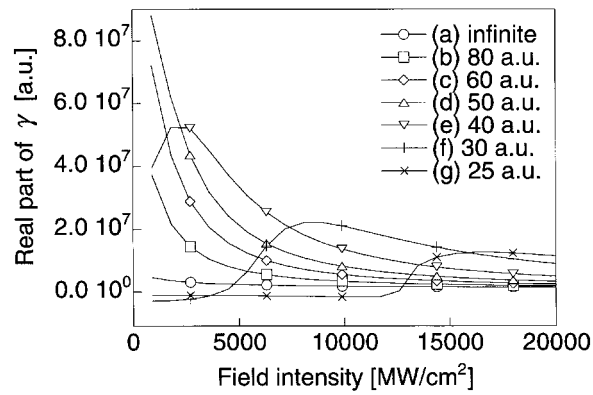

FIGURE 4. Variations in second hyperpolarizability γ for the dimer model with $\theta = 90°$ (Fig. 3) as a function of the intensity of the external electric field. The frequency of the field is 37,787 cm^{-1} as compared to the one-photon resonant value of 37,800 cm^{-1}. Results are shown at seven intermolecular distances: (a) infinite, (b) 80 a.u., (c) 60 a.u., (d) 50 a.u., (e) 40 a.u., (f) 30 a.u., and (g) 25 a.u.

in the induced field $\mathbf{E}^{(\zeta\zeta')}$ describing the intermolecular interaction seems to be related to the changes of the resonance frequency and the γ spectral shape, which causes the abrupt increase behaviors. In order to elucidate these effects, we next investigate the γ spectra of this dimer model for various field intensities and intermolecular distances.

DEPENDENCES OF γ SPECTRUM IN ONE-PHOTON RESONANT REGION FOR DIMER MODEL ON INTERMOLECULAR DISTANCES AND FIELD INTENSITIES

In this section, we investigate the dependences of γ spectra in one-photon resonant region for the dimer model shown in Figure 3 on the intermolecular distances and the field intensities. The real part spectra of γ for the dimer model are shown in Figure 5. Results are shown at seven intermolecular distances: (a) infinite, (b) 80 a.u., (c) 60 a.u., (d) 50 a.u., (e) 40 a.u., (f) 30 a.u., and (g) 25 a.u. We employ five types of intensities for external electric fields (90, 900, 1800, 4500, and 9000 MW/cm^2). All the fields have the same frequency (37,787 cm^{-1}) as compared to the one-photon resonant frequency (37,800 cm^{-1}) for the one-molecular two-state system.

Similar to the α spectra observed in our previous study [7], the resonance frequency (37,800 cm^{-1} for the one-molecule) at the same field intensity is found to be shifted to a higher-frequency region, as the intermolecular distance is reduced. This feature corresponds to the phenomenon observed in the H ($\theta = 90°$) aggregate. Such phenomenon is usually analyzed by using the dipole–dipole coupling [4]. Namely, the sign of the dipole–dipole interaction is determined by the angle θ among the parallel dipoles and the longitudinal axis, and the intermolecular distance affects the shift of the transition energy. For $\theta = 90°$ (H aggregate), the transition energy is known to become larger than that in the case without dipole–dipole coupling. It is also noted that the spectral peak in the frequency region below the resonance frequency is enhanced, as the intermolecular distance is reduced. This feature supports the increase in the γ values for cases (a)–(e) (shown in Fig. 4) with the decrease in the intermolecular distances in the low field-intensity region.

The intensity of the field is shown to change both the resonance frequency and the spectral line shape around the resonance region. The resonance frequency is found to be shifted to a lower-frequency region, as the field intensity increases. For cases (f) and (g) with intermolecular distances less than 40 a.u., original resonance peaks are found to be shifted to a higher-frequency region, e.g., in the case of (g), 4.0×10^4 cm^{-1} at 90 MW/cm^2. Further, a new sharp resonance peak with negative γ value appears above the original resonance frequency (37,800 cm^{-1}). This new resonance peak is also found to be shifted to a lower-frequency region, as the field intensity increases. The pass of this resonance frequency over the incident-field frequency (37,787 cm^{-1}) with the increase in the field intensity enhances the γ abruptly. This feature causes the abrupt changes of γ values for cases (f) and (g) around 5.0×10^3 and 1.3×10^4 MW/cm^2, respectively (see Fig. 4).

VARIATIONS IN γ IN THREE-PHOTON RESONANT REGION OF A DIMER MODEL FOR INTERMOLECULAR DISTANCES AND FIELD INTENSITIES

In this section, the feature of a three-photon resonance process, which is important in THG, is considered. We investigate the γ of a dimer model composed of the three-state one-molecule systems (Fig. 6), which mimic the electronic states of allyl cation [20]. It is found that this system exhibits off-resonant negative γ value [20], which is rare in organic nonlinear optical molecules. The damping factor Γ_{ii} is determined by an energy-dependent relation: $\Gamma_{ii} = fE_{j1}(f = 0.02)$ [19]. The external single-mode laser has a frequency (16,038 cm^{-1}) as compared to the three-photon resonant frequency (16,097 cm^{-1}) for the three-state one-molecule model. The division number of the one optical cycle of the external field is 1000, and the γ is calculated by using the Fourier transformation of polarization for 100 optical cycles after nonstationary time evolution (400 cycles). Similarly to the one-photon resonance case, we consider a case of angle 90° between the dipole for each molecule and the longitudinal axis.

The dependence of the γ on the applied field intensities are investigated. Figure 7 shows the results at four intermolecular distances: (a) infinite, (b) 30 a.u., (c) 25 a.u., and (d) 20 a.u. The result of case (a) is obtained by using noninteracting dimer model. As shown in Figure 7, the γ values are found to be negative for all the inter-

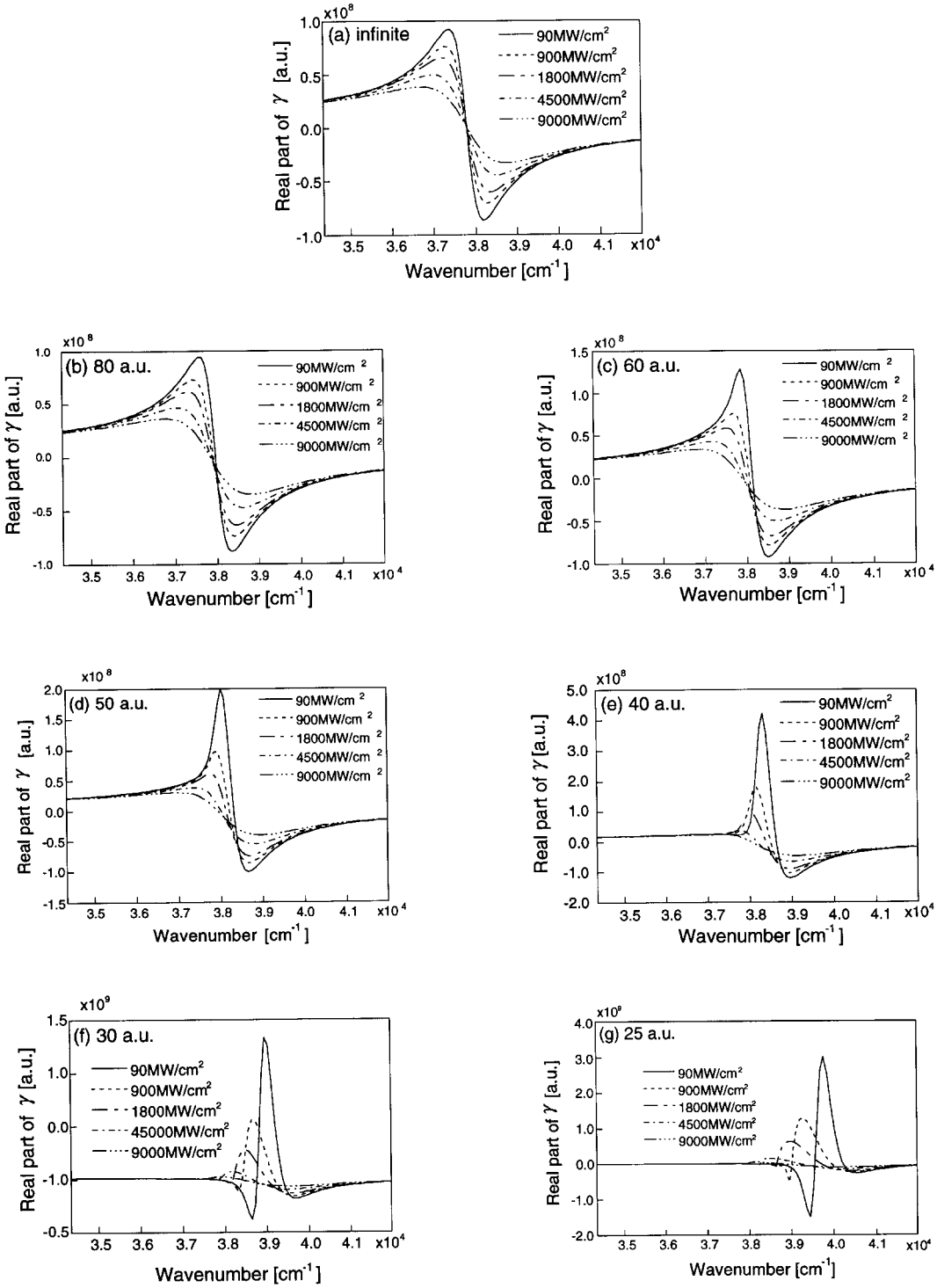

FIGURE 5. Real part of spectra of second hyperpolarizability γ for the dimer model [$\theta = 90°$; see Fig. 3(b)]. Results are shown at seven intermolecular distances: (a) infinite, (b) 80 a.u., (c) 60 a.u., (d) 50 a.u., (e) 40 a.u., (f) 30 a.u., and (g) 25 a.u. Five types of intensities for external electric fields (90, 900, 1800, 4500, and 9000 MW / cm^2) are employed. The frequencies of these fields are the same value, 37,800 cm^{-1}, as compared to the one-photon resonant value of 37,800 cm^{-1}.

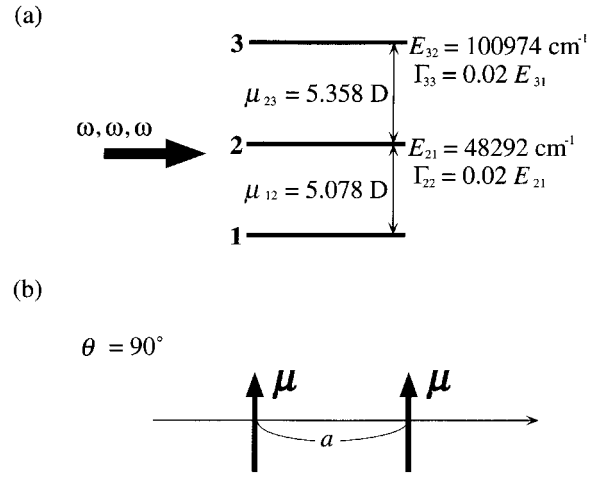

FIGURE 6. Three-state model [constructed from ground (**1**) and the excited (**2**, **3**) states] for (a) one-molecule system. (b) The dimer with $\theta = 90°$ is considered. The transition moments and transition energies between states i and j are described by μ_{ij} and E_{ji}, respectively. The damping factor is $\Gamma_{jj} = fE_{j1}$ ($f = 0.02$).

molecular distances and field intensities considered in this study. In contrast to the case of one-photon resonance case, the γ values for cases (a)–(d) do not show phase transition-like abrupt changes as the field intensity increases. For all cases, it is found that the $|\gamma|$ values increase to a maximum point and then decrease as the field intensity increases. As the intermolecular distance is smaller, the maximum point is found to be moved to the lower frequency region.

It is well-known that the population of the excited state appears in the case of one-photon resonance, while it is negligible in the case of three-photon resonance. Considering from the intensity–dependences of one- and three-photon resonant γ, the appearance of population in the excited state is presumed to be essential for the abrupt changes of γ, in addition to the retarded intermolecular interaction.

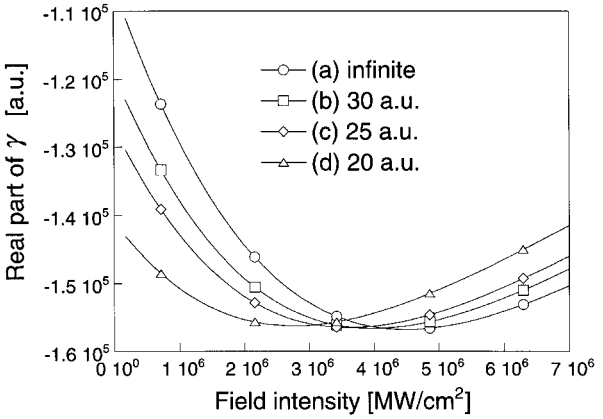

FIGURE 7. Variations in second hyperpolarizability γ for the dimer model with $\theta = 90°$ (Fig. 6) as a function of the intensity of the external electric field. The frequency of the field is 16,038 cm^{-1} as compared to the one-photon resonant value of 16097 cm^{-1}. Results are shown at seven intermolecular distances: (a) infinite, (b) 30 a.u., (c) 25 a.u., and (d) 20 a.u.

DEPENDENCES OF γ SPECTRUM IN THREE-PHOTON RESONANT REGION FOR A DIMER MODEL ON INTERMOLECULAR DISTANCES AND FIELD INTENSITIES

In this section, we investigate the dependences of γ spectrum for the dimer model shown in Figure 6 on the intermolecular distances and the field intensities. The real part spectra of γ for the dimer model are shown in Figure 8. Results are shown at four intermolecular distances: (a) infinite, (b) 30 a.u., (c) 25 a.u., and (d) 20 a.u. We employ three types of intensities for external electric fields (1,080,000, 3,060,000, and 7,020,000 MW/cm^2). All the fields have the same frequency (16,038 cm^{-1}) as compared to the three-photon resonant frequency (16,097 cm^{-1}) for the one-molecular three-state system.

Similarly to the γ spectra of the dimer composed of two-state molecules in the previous section, the resonance frequency (16097 cm^{-1} for the one-molecule) at the same field intensity is found to be shifted to higher-frequency region, as the intermolecular distance is reduced. However, this shift is found to be much smaller than that observed in the one-photon resonant γ spectra in the previous section. This is why the intermolecular interaction of the dimer in this section is much smaller than that in the previous section, since the transition moment between the ground and the excited states for the present three-state molecule shown in Figure 6 is much smaller than that for the previous two-state molecule shown in Figure 3.

Similarly to the γ spectra of the dimer composed of two-state molecules in the previous section, the intensity of the field is shown to change

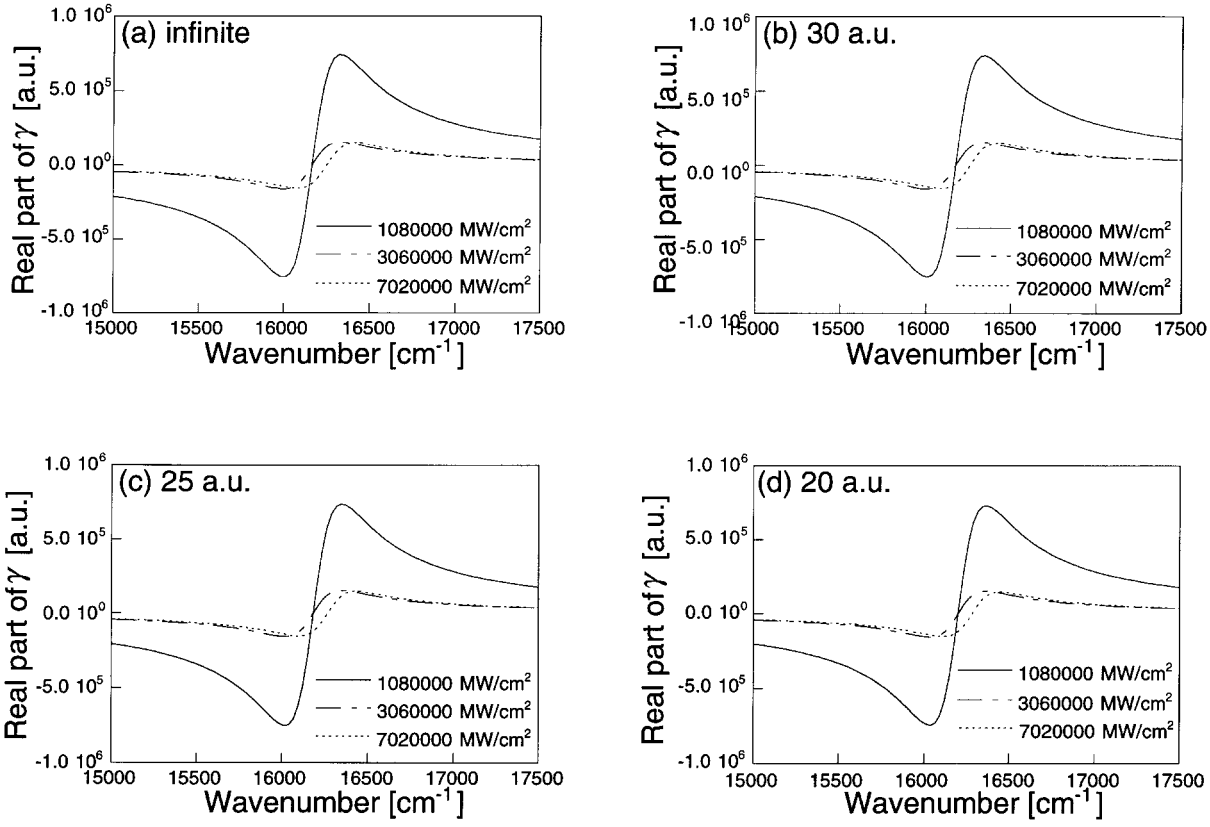

FIGURE 8. Real part of spectra of second hyperpolarizability γ for the dimer model [$\theta = 90°$; see Fig. 6(b)]. Results are shown at four intermolecular distances: (a) infinite, (b) 30 a.u., (c) 25 a.u., and (d) 20 a.u. Three types of intensities for external electric fields 1,080,000, 3,060,000 and 7,020,000 MW / cm^2) are employed. The frequencies of these fields are the same value, 16,038 cm^{-1}, as compared to the one-photon resonant value of 16097 cm^{-1}.

the three-photon resonance frequency and reduce the magnitude of γ, while the spectral line shape around the three-photon resonance region does not change remarkably in contrast to the case of the one-photon resonance shown in Figure 5. Further, as the intensity of the field increases, the three-photon resonance frequency is found to be shifted to a higher-frequency region against the case of one-photon resonance shown in Figure 5. There are also no additional resonance peaks around the original resonance frequency. The pass of the negative peak of real γ spectra over the incident-field frequency (16,038 cm^{-1}) and the reduction of $|\gamma|$ with the increase in the field intensity cause the continuous change in the intensity dependence of γ shown in Figure 7. From the results of one- and three-photon resonances, the feature that there are no remarkable changes in the shape of γ spectra seems to be related to the population change in the first excited states. Namely, the emergence of population in the excited state is expected to be essential for the abrupt changes in the field-intensity dependence of γ.

Conclusions

In this study, we developed a novel numerically exact calculation method of second hyperpolarizability (γ) spectrum for a linear aggregate including M-state molecules. This method has the advantage of treating the optical retardation effects, which are important to correctly describe molecular interactions in the wave zone [8]. As examples, we investigated γ for two- and three-state dimer models with 90° between the molecular dipole and the longitudinal axis, under the intense electric fields, respectively, with near one-photon and near three-photon resonant frequencies for the one-molecule system. In case of dimers composed of two-state molecules with small intermolecular dis-

tances under near one-photon resonant electric field, the γ values showed abrupt changes at the high-field intensity, similarly to the behavior of population difference and polarizability of a dimer under a near one-photon resonant field [7]. In contrast, in case of dimers composed of three-state molecules under near three-photon resonant electric fields, there are no phase transition-like abrupt changes when the field intensity increases, and is just only a continuous behavior of intensity dependence of γ. It is found for the intensity and intermolecular distance dependencies of γ spectra that in the one-photon resonant case, a shift, a shape change, and a new appearance of resonance peak of γ occur, while in the three-photon case only a shift of resonance peak of γ occurs. Considering these results, the appearance of population in the excited state seems to play an important role for abrupt changes of γ, in addition of the retarded intermolecular interaction. Unfortunately, although any experimental and theoretical results which can be compared with our present results do not exist now, we might propose some experiments to probe the present abrupt change in third-order response. For example, a measuring the field intensity dependence of third-order susceptibility for the linear aggregate thin layer in the one-photon resonant spectral region could elucidate the abrupt change for a given value of the incident light intensity.

The NCLA is expected to be useful for the investigation of the high-order polarizations of intermediate- and large-size linear aggregates constructed from arbitrary number of states under various time-dependent external fields. Further, the NCLA can be easily extended to the case with two- and three-dimensional optically retarded intermolecular interactions. It is interesting to investigate the field-intensity and molecular-size dependencies of multiphoton processes for various intermediate- and large-size molecular aggregates.

ACKNOWLEDGMENTS

This work was supported by a grant from the Ministry of Education, Science and Culture of Japan (Scientific Research on Priority Areas, No. 09241218 and No. 10149101) and a Grant from INAMORI Foundation.

References

1. Bloembergen, N. Nonlinear Optics; Benjamin: New York, 1965.
2. Shen, Y. R. The Principles of Nonlinear Optics; Academic: New York, 1984.
3. Kanis, D. R.; Ratner, M. A.; Marks, T. J. Chem Rev 1994, 94, 195.
4. Spano, F. C.; Knoester, J. Adv Magn Opt Res 1994, 18, 117.
5. Stroud, C. R.; Eberly, J. H.; Lama, W. L.; Mandel, L. Phys Rev A 1972, 5, 1094.
6. Bowden, C. M.; Sung, C. C. Phys Rev A 1979, 19, 2392.
7. Nakano, M.; Yamaguchi, K. Int J Quant Chem, to appear.
8. Craig, D. P.; Thirunamachandran, T. Molecular Quantum Electrodynamics; Academic: New York, 1984.
9. Malyshev, V.; Moreno, P. Phys Rev A 1996, 53, 416.
10. Shirley, J. H. Phys Rev B 1965, 138, 979.
11. Wang, K.; Chu, S.-I. J Chem Phys 1987, 86, 3225.
12. Kavanaugh, T. C.; Silbey, R. J. J Chem Phys 1992, 96, 6443.
13. Hirshfelder, J. O.; Wyatt, R. E.; Coalson, R. D. Lasers, Molecules and Methods; Wiley: New York, 1989.
14. Nakano, M.; Yamaguchi, K. Phys Rev A 1994, 50, 2989.
15. Tan-no, N.; Ohkawara, K.; Inaba, H. Phys Rev Lett 1981, 46, 1282.
16. Samoc, M.; Prasad, P. N. J Chem Phys 1989, 91, 6643.
17. Born, M.; Wolf, E. Principles of Optics; Pergamon: Oxford, 1980.
18. Nakano, M.; Yamaguchi, K.; Matuzaki, Y.; Tanaka, K.; Yamabe, T. Chem Phys 1995, 102, 2986.
19. Shuai, Z.; Brédas, J. L. Phys Rev B 1991, 44, 5962.
20. Nakano, M.; Yamada, S.; Shigemoto, I.; Yamaguchi, K. Chem Phys Lett 1996, 251, 381.